



Published in final edited form as:

Biomaterials. 2013 May ; 34(16): 3970–3983. doi:10.1016/j.biomaterials.2013.01.045.

Highly elastomeric poly(glycerol sebacate)-co-poly(ethylene glycol) amphiphilic block copolymers

Alpesh Patel^{#1,2}, Akhilesh K. Gaharwar^{#3,4}, Giorgio Iviglia^{#1,2,5}, Hongbin Zhang^{1,2,6}, Shilpaa Mukundan^{1,2}, Silvia M. Mihaila^{1,2}, Danilo Demarchi^{5,7}, and Ali Khademhosseini^{1,2,4,*}

¹Center for Biomedical Engineering, Department of Medicine, Brigham and Women's Hospital, Harvard Medical School, Cambridge, MA 02139 (USA)

²Harvard-MIT Division of Health Sciences and Technology, Massachusetts Institute of Technology, Cambridge, MA 02139 (USA)

³Wyss Institute for Biologically Inspired Engineering, Harvard University, Boston, MA 02115 (USA)

⁴David H. Koch Institute for Integrative Cancer Research, Massachusetts Institute of Technology, Cambridge, MA 02139 (USA)

⁵Department of Electronics and Telecommunications, Politecnico di Torino, Torino 10129 (Italy)

⁶School of Materials Science and Engineering, University of Science and Technology, Beijing, Beijing, 100083 (China)

⁷Center for Space Human Robotics, Italian Institute of Technology, Torino (Italy)

These authors contributed equally to this work.

1. INTRODUCTION

Development of biodegradable materials has stimulated interest in a range of biotechnological and biomedical applications.[1-5] Amongst them, synthetic biodegradable polymers have been extensively investigated owing to their tunable physical and chemical properties, low batch-to-batch variation, ease of fabrication and modification, and low risk of disease transmission.[6-10] In last few years, several biodegradable polymers such as poly(lactic acid) (PLA), poly(glycol acid) (PGA), poly(ϵ -caprolactone) (PCL), poly(hydroxybutyrate) (PHB) and their block copolymers have been explored for development of emerging technologies in biomedical and biotechnological industries. [10-12] This is mainly attributed to their high mechanical strength, and *in vivo* biocompatibility. Despite the interesting physical and chemical properties, some of these

* alik@rics.bwh.harvard.edu (Prof. A. Khademhosseini).

Authors Contributions

AP, AKG and AK conceived the idea and designed the experiments. AP, AKG and GI synthesized PGS and PGS-co-PEG polymers and performed the chemical (NMR, FTIR, GPC), mechanical (tensile, compression and cyclic testing), and structural characterizations (sol-gel, hydration kinetics, contact angle, degradation studies). SMM performed cells proliferation studies. HZ and SM performed protein adsorption studies. AP, AKG, GI and AK analyzed experimental data and wrote the manuscript. All authors discussed the results and commented on the manuscript.

polyesters create an acidic local environment upon degradation that causes an inflammation to the surrounding tissues.[10, 13] Moreover, the conventional polyesters follow the bulk degradation mechanism and display exponential decay in their mechanical properties with degradation.[14]

Poly(glycerol sebacate) (PGS), a tough elastomer, has been proposed for tissue engineering applications due to controlled and linear degradation profiles.[14-16] The surface erodible nature of PGS makes it preferable and unique over the other polyesters for controlled drug delivery and scaffolding applications.[16-20] The elastic modulus of PGS can be easily tuned by controlling various parameters such as reaction time, reaction temperature and time of curing.[16] Additionally, both the reactants glycerol and sebacic acid, used in the synthesis of PGS are inexpensive and approved by FDA for biomedical applications.[21-23] As a result, PGS have been explored for numerous tissue engineering applications such as myocardial tissue[24], vascular graft[25], cartilage tissue[26], nerve guide[27], retinal transplantation[28], surgical sealant[29].

To incorporate different functionalities and tailor physiochemical properties for specific tissue engineering applications, various PGS based copolymeric systems and blends were developed.[15, 29, 30] For example, lactic acid was incorporated within the PGS backbone and a range of copolymers were developed by varying the molar ratio of glycerol, sebacic acid and lactic acid.[31] They demonstrated that the addition of lactic acid resulted in the increased mechanical properties and decreased degradation rates.[31] However, with an increase in lactic acid concentration, the surface degradation characteristic of PGS was compromised with the bulk erosion behavior.[31, 32] In another study, Sun *et al.* developed poly(glycerol sebacate)-*co*glycolic acid (PGS-*co*-GA) with different reactant ratios and showed that the addition of glycolic acid decreases the elastic modulus, whereas the degradation rate increases exponentially with the addition of glycolic acid.[32] Most of these studies aimed at tuning either the degradation behavior or the mechanical properties of PGS with a very limited focus on improving the hydration properties.

Hydration properties of biomaterials is an important parameter for tissue engineering applications as it directly determines the mechanical stability, degradation rate, and diffusion characteristic of the scaffolds under dynamic *in vivo* conditions.[33-35] For example, water uptake within a tissue engineered scaffold should be high enough to promote the mechanical deformation with minimum hysteresis under dynamic/cyclic stresses.[33, 34] Moreover, the water uptake and diffusion characteristics of polymeric scaffolds also decide the degradation mechanism of scaffolds as well as cellular behavior.[13, 36] For these reasons, there is a need to better control hydration properties of PGS to tailor the mechanical properties, and degradation characteristic.

Recently, Liu *et al.* incorporated citric acid within PGS backbone to increase the hydrophilicity of the developed poly(sebacate-glycerol-citrate) (PGSC) copolymers.[37] The presence of additional carboxyl groups present on the citric acid enhances the water uptake ability of the PGSC.[37] Another approach to tune the hydration property of polyesters is to design polyether-polyester amphiphilic block copolymers.[9, 38] A range of polyesters such

as PCL, PGA, PLGA, PLA and PHB, have been copolymerized with polyethylene glycol (PEG), a polyether, to tune swelling degrees.[39]

Here, we report synthesis and fabrication of amphiphilic, biodegradable block copolymer from PGS and PEG. We hypothesized that the incorporation of PEG segments within PGS backbone will allow us to tune the hydrophilicity while maintaining the controlled degradation behavior of PGS. A range of PGS-*co*-PEG polymer from mechanically stiff to elastomeric soft was synthesized. The effect of addition of PEG to PGS on hydration properties was monitored by hydration kinetics and contact angle measurements. The elastomeric properties of the copolymers were studied by uniaxial tensile, unconfined compression, cyclic tensile and cyclic compression testing. *In vitro* behaviors of PGS-*co*-PEG polymers were evaluated by degradation rate, protein adsorption/absorption and cell adhesion properties. We aim to create PGS based amphiphilic block copolymer with tailored chemical and physical properties for a wide range of biomedical and biotechnological applications.

2. MATERIALS AND METHODS

2.1 Synthesis of poly (glycerol sebacate) (PGS)

The PGS pre-polymer was synthesized by polycondensation of equimolar glycerol (Sigma-Aldrich, Milwaukee, WI) and sebacic acid (Sigma-Aldrich) according to previously published methods.[16] Briefly, an equimolar amount of glycerol and sebacic acid were melted and stirred for 2 hours in a 250 mL two necked round bottom reactor under Argon at 130 °C. The reaction pressure was slowly reduced to 50 mTorr over 5 hours and the reaction was continued under vacuum for another 48 hours at 130 °C. The prepolymer samples were collected for spectroscopic analysis. The remaining prepolymer was poured into Teflon crucibles and thermally cured in the vacuum oven at 130 °C for 48 hours.

2.2 Synthesis of poly (glycerol-sebacate)-*co*-polyethylene glycol (PGS-*co*-PEG polymer)

PGS-*co*-PEG pre-polymers were synthesized via two steps condensation polymerization. The first step involved the polycondensation of sebacic acid and polyethylene glycol (Alfa Aesar, Mw=1000 g/mol) under stirring condition. PEG was dried in vacuum chamber at 90 °C before its use. The reaction was then carried out at 130 °C under the flow of Argon for 2 hours and under vacuum of 50 mTorr for another 24 hours. In the second step, specific amount of glycerol was added into the reactor, mixed thoroughly under the flow of Argon and the reaction was further carried out at 130 °C under reduced pressure of 50 mTorr for 48 hours. The samples of pre-polymers were collected for spectroscopic analysis. The viscous pre-polymer solutions were poured in Teflon crucibles and thermally cured in the vacuum oven at 130 °C for 48 hours. The overall diol to dicarboxylic acid molar ratio was kept constant. Three molar ratios of PEG to glycerol (20/80, 40/60 and 60/40) were used to develop PGS-*co*-PEG polymer with different degree of PEG segment within copolymer system.

2.3 Chemical Characterization

The molecular weight of pre-polymer of PGS and PGS-*co*-PEG polymer was determined using gel permeation chromatography (GPC, Waters, Milford, MA). The samples were dissolved in tetrahydrofuran (THF) (0.5 % w/v) and injected at the flow rate of 1 mL/min. The polystyrene standards were used for the calibration. Fourier Transform Infrared (FTIR) spectra of the samples were recorded using Alpha Bruker spectrometer. The average value of 48 scans at 4 cm⁻¹ resolutions were collected for each sample. The FTIR spectra were analyzed for PGS and PGS-*co*-PEG polymer before and after thermal curing. The pre-polymer samples of PGS and PGS-*co*-PEG polymer were also analyzed using Nuclear magnetic resonance (¹H-NMR) spectroscopy (Varian Inova 500). The pre-polymer samples were dissolved in CDCl₃ and the spectra were recorded at 500 MHz. The resulting data were processed and analyzed using ACDLABS/1D NMR software. The peak assignment in the NMR spectra for PGS and PGS-*co*-PEG pre-polymers are listed below. ¹H-NMR (PGS) (500 MHz, CDCl₃) δ/ppm: 1.30 (37H, m, -CH₂-), 1.62 (18H, d, -CH₂CH₂O(CO)-), 2.35 (18H, m, -CH₂O(CO)-), 3.50-3.85 (6H, m, OHCH₂CHO-), 3.94 (1H, m, -OCH₂CHOH), 4.05-4.35 (15H, m, -OCH₂CHO-), 5.09 (1H, s, OHCH₂CHO-), 5.26 (1H, s, -OCH₂CHO-). ¹H-NMR (PGS-20PEG) (500 MHz, CDCl₃) δ/ppm: 1.30 (12H, m, -CH₂-), 1.62 (6H, d, -CH₂CH₂O(CO)-), 2.35 (6H, m, -CH₂O(CO)-), 3.64 (25H, m, -OCH₂-), 3.94 (1H, m, -OCH₂CHOH), 4.05-4.35 (5H, m, -OCH₂CHO-), 5.09 (1H, s, OHCH₂CHO-), 5.26 (1H, s, -OCH₂CHO-). ¹H-NMR (PGS-40PEG) (500 MHz, CDCl₃) δ/ppm: 1.30 (19H, m, -CH₂-), 1.62 (9H, d, -CH₂CH₂O(CO)-), 2.35 (9H, m, -CH₂O(CO)-), 3.64 (76H, m, -OCH₂-), 3.94 (1H, m, -OCH₂CHOH), 4.05-4.35 (6H, m, -OCH₂CHO-), 5.09 (1H, d, OHCH₂CHO-), 5.26 (1H, s, -OCH₂CHO-). ¹H-NMR (PGS-60PEG) (500 MHz, CDCl₃) δ/ppm: 1.30 (14H, m, -CH₂-), 1.62 (7H, d, -CH₂CH₂O(CO)-), 2.35 (7H, m, -CH₂O(CO)-), 3.64 (85H, m, -OCH₂-), 3.94 (1H, m, -OCH₂CHOH), 4.05-4.35 (4H, m, -OCH₂CHO-), 5.09 (1H, s, OHCH₂CHO-), 5.26 (1H, s, -OCH₂CHO-).

The degree of crosslinked network was determined by evaluation sol and gel contents analysis. Here, samples (4 mm in diameter, 1.2-1.9 mm thickness and initial weight (W_o)) were allowed to swell in *tetrahydrofuran* (THF) for 24 hours to elute out the sol contents. The remaining gel contents were weighed after drying (W_d) the sample overnight. The percentage of sol contents was calculated by Eq. (1).

$$Sol \quad (\%) = \frac{(W_o - W_d)}{W_o} \times 100 \quad \text{Eq. (1)}$$

2.4 Mechanical Properties

The mechanical properties of PGS and PGS-*co*-PEG polymer were evaluated using uniaxial tensile, unconfined compression, cyclic tensile and cyclic compression testing using Instron 5943 Materials Testing System Capacity (Norwood, MA, USA) equipped with 50 N load cell. For uniaxial tensile and cyclic tensile testing, thermally crosslinked samples were cut in a rectangular shape with 10 mm gauge length, 5 mm wide and approximately 1.2-1.9 mm thick. The mechanical properties were performed in both as-prepared and hydrated conditions (soaked in PBS at 37 °C for 24 hours). For uniaxial tensile test, samples were

stretched until failure at the crosshead speed of 10 mm/min. Force-displacement curves that is obtained from the machine were converted to stress-strain curves. The stress (σ_{tens} , MPa) was obtained by dividing the applied force (N) with cross section area (mm^2) and strain was obtained from the displacement using $((L-L_0) \times 100 / (L_0))$, where L_0 was initial gauge length and L was instantaneous gauge length. Young's Modulus was calculated from the linear stress-strain region by fitting a straight line between 5 to 15% strain and toughness of the copolymer network was determined by total area under the stress-strain curve. The ultimate tensile stress, fracture stress and failure strain were also calculated. The uniaxial compression testing was performed with a crosshead speed of 1 mm/min on circular samples with 4 mm in diameter and 1.2-1.9 mm thickness. The 5-15% strain region was used to measure the compressive modulus of the samples and instantaneous drop in more than 20% stress was considered as a fracture point.

For cyclic testing, 5 loading and unloading cycles were performed between 0-20 % strain. To emphasize the elastic behavior of the copolymer network, the cyclic stress-strain curves (tensile and compression) were represented in Mooney-Rivlin plot using Eq (2) and Eq. (3). [40] For tensile test, the Mooney's stress (σ_{Mooney}) is plotted as a function of $1/\lambda_{tens}=L/L_0$, where L is the instantaneous gauge length and L_0 is the initial gauge length, and the Mooney' stress (σ_{Mooney}) was calculated as follows [40-42]:

$$\sigma_{Mooney} = \frac{\sigma_{tens}}{\lambda_{tens}^4 - \frac{1}{\lambda_{tens}^2}} \quad \text{Eq. (2)}$$

For compression test, compressive stress (σ_{comp} , MPa) is obtained by dividing applied force (N) by cross-section area (mm^2). Mooney's stress is plotted as a function of $1/\lambda_{biax}$, where λ_{biax} is defined as $1/\lambda_{comp}$ and $\lambda_{comp}=h/h_0$ (h_0 is the initial height and h is the current height of the sample). Mooney stress was calculated as follow [40-42]:

$$\sigma_{Mooney} = \frac{\sigma_{Comp}}{\lambda_{Comp} - \frac{1}{\lambda_{Comp}^2}} = \frac{\sigma_{Comp}}{\lambda_{biax}^4 - \frac{1}{\lambda_{biax}^2}} \quad \text{Eq. (3)}$$

2.5 Hydration Properties and Physiological Stability

The hydration properties of copolymeric network were determined by contact angle measurements, and hydration kinetics. The contact angle of water on crosslinked samples was measured by Dynamic Contact Angle Analyzer (Kruss-DSA-100) using sensible drop method ($n=5$). A droplet of de-ionized water was deposited on the sample film using 21-gauge needle and high-resolution image of the droplet was captured after 10 sec. For hydration kinetic, samples (4 mm diameter, 1.2-1.9 mm thickness and W_0 (initial weight)) were allowed to swell in physiological conditions (37°C in Dulbecco's phosphate buffer saline (PBS)). The swollen disks were taken out of the PBS at regular time intervals, blotted with a filter paper to remove excess surface water, and their swollen weights (W_s) were noted. The water uptake by the polymeric network was determined by Eq. (4):

$$\text{Hydration Degree (\%)} = \frac{(W_s - W_o)}{W_s} \times 100 \quad \text{Eq. (4)}$$

The physiological stability of copolymeric network was investigated by *in vitro* degradation studies. The sample discs (4 mm diameter and 1.2-1.9 mm height) were immersed in PBS at 37 °C after recording their initial weight (W_o). The degradation study was carried out for 21 days where the samples were taken out at specific time intervals, dried overnight and weighed (W_f). The mass loss was calculated using Eq. (5):

$$\text{Mass Loss (\%)} = \frac{(W_o - W_f)}{W_o} \times 100 \quad \text{Eq. (5)}$$

2.6 Protein Adsorption/Absorption

Sample disks (n=3) of PGS and PGS-*co*-PEG polymers (20%, 40% and 60% PEG) having 4 mm diameter were soaked at 37 °C in PBS for 24 hours. The PBS was aspirated and disks were soaked in 500 μ l of protein solution for 24 hours at 37 °C. For protein adsorption from fetal bovine serum (FBS, Gibco, USA), 10 % (v/v) FBS in 1 \times PBS was used whereas for fibronectin adsorption study 50 μ g/mL of fibronectin in 1 \times PBS was used. The samples were then washed 3 times in PBS to extract any non-specific adsorbed proteins. The samples were then treated with 2 % SDS solution for 6 hours in a shaker maintained at 50 rpm to extract the adsorbed proteins. The supernatant was collected separately by centrifuging the samples and the eluted protein were analyzed using micro Bicinchoninic acid (BCA) protein assay reagent (Pierce BCA, Thermo Scientific) and quantified using a UV/Vis spectrophotometer (Epoch Biotech Instruments) at 562 nm.

2.7 In vitro Studies

The cell adhesion properties of the polymer were assessed by seeding NIH 3T3 fibroblast cells on different compositions of PGS-*co*-PEG polymers. Briefly, the cells were cultured in Dulbecco's Modified Eagle Medium (DMEM, Gibco, USA), supplemented with 10 % FBS, and 1 % antibiotic (penicillin/streptomycin, Gibco, USA), in a humidified atmosphere with 5 % of CO₂, at 37 °C. When the culture reached 80 % confluence, the cells were trypsinized (0.05 % Trypsin/EDTA, Gibco, USA) from the tissue culture flask, subsequently re-suspended in culture medium and seeded on PGS-*co*-PEG polymers at a density of 5 \times 10⁵ cells per sample in a low cell-adhesive 24-well plate. Cells were allowed to adhere for 1 hour and then 500 μ L of medium was added. The proliferation rate of the adhered cells on day 1, 4 and 10 was assessed using an AlamarBlue assay (Invitrogen) following standard protocol. Tissue culture polystyrene (TCPS) surface was used as a positive control.

2.8 Statistics

Experimental data were presented as mean \pm standard deviation. Statistical differences between the groups were analyzed using one-way ANOVA using Tukey post-hoc analysis and two-way ANOVA. Statistical significance was represented as *p<0.05, **p<0.01, ***p<0.001.

3. RESULTS AND DISCUSSION

3.1 Synthesis of PGS-co-PEG polymers

The synthesis of PGS-co-PEG polymers was performed in three steps (Figure 1a). In the first step, polycondensation reaction of PEG and sebacic acid was carried out in order to get a linear prepolymer chain and to avoid any crosslinking. In the second step, glycerol was added to obtain a block copolymer of PGS-co-PEG (pre-polymer) with different ratio of PEG segments. In the third step, the pre-polymer was thermally crosslinked. The crosslinking density of the pre-polymers can also be altered by varying the time and temperature of curing[15], however the curing conditions were kept constant in this study to investigate the effect of PEG on PGS network.

A series of PGS-co-PEG polymers was designed by altering the glycerol/PEG molar ratios. The nomenclature of synthesized PGS-co-PEG polymers was based on the glycerol/PEG molar ratios and was represented as PGS-co-xPEG, where “x” represents the molar concentration of PEG within the PGS. For example, the PGS-co-20PEG represents the copolymer with 20% PEG and 80% PGS. The hydrophilicity of the final block copolymer was tuned by adding PEG in three different ratios (20%, 40% and 60%). The presence of PEG chains within materials increases hydrophilic nature (Figure 1b). Furthermore, the hydrophilic nature of copolymer network will facilitate the hydrolysis of ester bond. Thus, it is expected that the chemical, mechanical and degradation properties can be tailored by altering the amount of PEG within PGS backbone.

3.2 Chemical Characterization of PGS-co-PEG Polymers

The structure of pre-polymer (after the second step of polycondensation) was investigated using ^1H NMR spectroscopy (Figure 2a and S1). In the ^1H NMR of PGS, the methylene peaks related to sebacic acid were identified at 1.30, 1.62 and 2.35 ppm, whereas peaks between 4.05-4.35 ppm and 5.05-5.30 ppm were observed for glycerol. The presence of an additional methylene peak from PEG segment was observed in the ^1H NMR spectra of PGS-co-PEG polymers, indicating the presence of PEG segment within prepolymer solution. The ratio of methylene hydrogen within PEG and sebacic acid were calculated from NMR data (Figure 2b). The experimental ratio from NMR correlates well with the theoretical estimation indicating close control over the polymer synthesis process. Furthermore, presence of ester bond in pre-polymer was investigated using Fourier transform infrared spectroscopy (FTIR). A very strong peak around 1730 cm^{-1} corresponds to the ester group was observed which proves that all the pre-polymer contain PGS (Figure S2).

The molecular weight of pre-polymer of PGS and PGS-co-PEG polymer was determined using gel permeation chromatography (GPC). The results indicates that the molecular weight (M_w) of PGS was 5,012 Da (polydispersity index (PDI) = 2.64). The addition of 20, 40 and 60 % PEG result in copolymer with M_w of 4,998 Da (PDI=1.48), 4,037 Da (PDI=1.42) and 3,789 Da (PDI=1.4) respectively. The addition of PEG results in formation of polymer with lower PDI, indicating close control over the condensation reaction.

A fully crosslinked copolymer was obtained by subjecting the pre-polymer solution to thermal curing process at $130\text{ }^\circ\text{C}$ for 48 hours. The additional hydroxyl groups (-OH)

present on PGS backbone react with unreacted sebacic acid to form crosslinked networks (Figure 3a). The effect of thermal crosslinking on the polymer chains was investigated by monitoring FTIR spectra before and after the curing process (Figure 3b). The results indicated that the peaks at 1350 cm^{-1} (-COOH) and 1100 cm^{-1} (-OH) decreased and the peak at 1150 cm^{-1} (-COO) increased after the thermal crosslinking process. These observations indicate success of the curing process that results in formation of covalently crosslinked network. The decrease in the area of hydroxyl peak at 3450 cm^{-1} further confirms the thermal crosslinking process.

The FTIR spectra of the cured PGS-co-PEG polymers were shown in Figure 3c. The reduction in the hydroxyl peak at 3500 cm^{-1} was observed with an increase in the PEG segment. In PGS, the ratio of methylene (-CH₂) peak to hydroxyl (-OH) peak was 3.57. The addition of PEG results in an increase in CH₂/OH ratio to 5.94, 7.39 and 7.5 for PGS-co-20PEG, PGS-co-40PEG and PGS-co-60PEG respectively. At higher PEG concentrations (40 and 60% PEG), the CH₂/OH ratio was very similar. This indicates that the number of additional hydroxyl groups were quite limited in copolymer containing above 60% PEG and result in lower crosslinking density.

The decrease in the crosslinking density due to the addition of PEG was also investigated by determining the sol content (unreacted pre-polymer) within the covalently crosslinked PGS-co-PEG polymer network. The presence of sol content within the crosslinked network was evaluated by swelling the network in tetrahydrofuran (THF). The high swelling degree of copolymers within THF allows the sol to diffuse-out. The gel content (crosslinked network) can be determined by obtaining the dry weight of remaining copolymer network (Figure S3). The results indicate that the thermally crosslinked PGS comprises of $9.9\pm 4.3\%$ sol content. The presence of low amount of sol content indicates high crosslinking density. This was mainly attributed to the presence of free hydroxyl groups on the polymer (PGS) backbone that can be used to form covalently crosslinked network. Addition of PEG decrease the amount of free hydroxyl group and thus a decrease in crosslinking density was observed. This was shown by an increase in the sol contents in PGS-co-PEG copolymers compared to PGS.

3.3 Highly Elastomeric and Tough PGS-co-PEG Polymers

Evaluation of new polymeric biomaterials for tissue engineering application requires extensive mechanical characterization under various *in vivo* conditions. Earlier studies reported that the mechanical properties of PGS could be tuned by changing the curing temperature and time.[15-17] For example, by increase the curing temperature of PGS from $110\text{ }^{\circ}\text{C}$ to $130\text{ }^{\circ}\text{C}$, Young's modulus, ultimate stress and elongation can be altered from 1.2 kPa to 56 kPa, 230 kPa to 470 kPa, and 448 % to 41 %, respectively. In our study, we used curing temperature of $130\text{ }^{\circ}\text{C}$ and curing time of 48 hours, and the mechanical properties of PGS reported here are similar to the previously published results.[17]

PGS is an elastomeric polymer[16], and addition of PEG further enhances its elastomeric properties (Figure 4). For example, PGS-co-PEG polymers can be subjected to serve deformation such as bending and stretching without fracturing the structure (Figure 4a). We investigated the mechanical properties of PGS and PGS-co-PEG polymer network using

uniaxial tensile test in dry (as-prepared) and hydrated conditions. From hydration kinetics data, we observed that addition of PEG to PGS significantly increases water uptake capacity of the copolymeric network. In order to evaluate the effect of water uptake on the tensile properties of the copolymeric network, we allowed the samples to hydrate in PBS for 24 hours and then subjected it to uniaxial tensile test. Figure 4b represents the stress-strain curve of PGS and PGS-co-PEG polymers in dry and hydrated conditions. The mechanical properties such as Young's modulus, ultimate stress, fracture stress and ultimate elongation were calculated from the stress-strain curves.

More than two-fold increase in elongation was observed due to addition of 60% PEG ($107.9 \pm 9.8\%$) when compared to pure PGS ($42.2 \pm 5\%$) in dry conditions (Figure 4d). Whereas, in fully hydrated conditions, almost six-fold increase in elongation was observed (PGS = $31.3 \pm 3.2\%$ and PGS-co-60PEG = $192.3 \pm 20\%$). This is mainly attributed to high water uptake capacity of PGS-co-PEG polymer that results in higher chain flexibility during mechanical deformation that facilitates chain elongation and deformation (Figure 4c).

The effect on the mechanical strength and the toughness of the material due to the addition of PEG to PGS was also investigated. (Figure 4e). In dry conditions, PGS has Young modulus, tensile strength and toughness of 2.39 ± 0.29 MPa, 690 ± 160 kPa and 190 ± 68 kJ/m³ respectively. The mechanical properties of PGS reported here are comparable to the previously published results.[16] The addition of PEG to PGS, significantly decreases the modulus, tensile strength and toughness. For example, addition of 60% of PEG to PGS decreases the Young's modulus, tensile strength and toughness to 40 ± 10 kPa, 26 ± 4 kPa and 17 ± 3 kJ/m³, respectively. This was mainly attributed to the decrease in crosslinking density due to reduction in hydroxyl groups present on PGS backbone.

It was observed that in PGS, both tensile strength (500 ± 76 kPa) and toughness (84 ± 26 kPa) decrease significantly without affecting the Young's modulus (2.26 ± 0.20 MPa) and elongation ($31.3 \pm 3.2\%$) when subjected to physiological condition. Whereas, more than three-fold decrease in modulus (13 ± 2 kPa) and two-fold (12 ± 2 kPa) decrease in ultimate strength was observed in PGS-co-60PEG compared to the dry conditions. In PGS, almost two-fold decrease in toughness was observed after hydration, whereas PGS-co-60PEG has very similar toughness in both dry and hydrated condition.

The previous study on mechanical properties on polyesters such as PLA, PLGA, PCL and co-polymers blended with PGS showed high mechanical properties in dry conditions, which drastically decreases after soaking in saline buffer or media.[30, 31] The change in the mechanical properties of the conventional polyesters in dry and wet conditions, create an inflammatory response that results in formation of fibrous capsule.[15] Moreover, high mechanical strength of these polymers/copolymers limit their application for soft tissue engineering (such as cartilage, cardiac, vocal fold), where good stiffness along with highly elastomeric properties are required.[15] Thus, it is essential to engineer stiff yet elastomeric biomaterials for soft tissue engineering. The PGS-co-PEG polymer network reported here have high stiffness along with elastomeric properties, make it suitable to engineer scaffolds for a range of soft tissues. For example, the tensile modulus of PGS-co-PEG polymers is

similar to human cardiac muscles (0.02–0.15MPa).[43, 44] Hence, PGS-*co*-PEG polymers can potentially be used to engineer cardiac patches.

3.4 Compressive Properties of PGS-*co*-PEG Polymers

PGS and PGS-*co*-PEG polymers display highly elastomeric properties under compressive deformation. The compressive properties of PGS and PGS-*co*-PEG polymers were investigated using unconfined compression testing. The compressive properties of PGS and PGS-*co*-PEG polymers were evaluated in dry (as prepared) and hydrated conditions (Figure 5a). The stress-strain curve of PGS indicates that the crosslinked network have similar compressive modulus in dry (6.70 ± 0.84 MPa) and hydrated (6.51 ± 0.47 MPa) conditions. Similarly, no significant difference in fracture strain, fracture stress and toughness was observed between dry and hydrated PGS samples (Figure 5b). As expected, with an increase in PEG content, the compressive modulus of PGS-*co*-PEG polymers decreases. However, no significant difference was observed for PEG-*co*-20PEG in dry and hydrated conditions. At higher PEG concentrations (PGS-*co*-40PEG and PGS-*co*-60PEG), significant decrease in modulus was observed in dry and hydrated samples. This can be mainly attributed to an increase in the water uptake ability of the copolymer at higher PEG content.

The fracture stress and fracture strain were only observed for PGS and PGS-*co*-20PEG samples, as the addition of more than 20 % PEG to PGS results in formation of highly elastomeric network that can sustain high compressive strain (more than 80% strain). Both PGS-*co*-40PEG and PGS-*co*-60PEG display a unique stress-strain behavior that is typically observed in highly elastomeric soft tissues (such as cartilage [45]). For example, PGS-*co*-60PEG displays a plateau at low strain (0-60 % strain) and almost vertical increase in stress was observed at higher strain (75-85 % strain). Moreover, compressive modulus of PGS-*co*-PEG polymers can be tuned between 3.2 MPa to 9 kPa by varying the PEG concentration, which is in the range of cartilage (0.4-0.8 MPa)[45].

3.5 Cyclic Tensile Properties of PGS-*co*-PEG Polymers

The applicability of PGS-*co*-PEG polymers to engineer elastomeric tissues that are subjected to repeating or pulsating *in vivo* mechanical forces, was investigated by evaluating the mechanical properties of the copolymeric network under cyclic tensile conditions. From the uniaxial tensile test, it was observed that, both PGS and PGS-*co*-PEG polymers display linear stress-strain curve until 20 % strain. We subjected the fully hydrated samples to 20 % cyclic tensile strain and monitored the loading and unloading stress-strain curve for five consecutive cycles. Pure PGS and PGS-*co*-PEG polymers showed elastomeric characteristic (Figure 6 and S4).

The area between the loading and unloading curve was used to determine the amount of energy absorbed by the crosslinked network and percentage recovery during the deformation cycle.[46, 47] Figure 6a shows that the addition of PEG significantly reduces the amount of energy absorbed (hysteresis). For example, PGS absorbs 6.17 ± 1.23 kJ/m³ during the first cycle and 2.33 ± 1.53 kJ/m³ during the fifth cycle, whereas PGS-*co*-60PEG absorbs 0.019 ± 0.006 kJ/m³ during the first cycle and 0.011 ± 0.004 kJ/m³ during the fifth cycle. Similar trend was observed for the recovery of the crosslinked network. After the first cycle,

PGS and PGS-*co*-PEG polymers show more than 90 % of recovery. These results indicate that the energy adsorbed (and recovery of network) in the first cycle was not equivalent to the subsequent cycles. This is mainly due to the plastic deformation of the crosslinked network during the first cycle. Whereas, the energy absorbed (and recovery of network) between second to fifth cycles was almost constant and can be attributed the elastic deformation of the network. This also indicates that after the first cycle, the crosslinked network showed little energy dissipation at the molecular level and the copolymer network had high recoverability.

The normal tensile stress-strain curves of PGS and PGS-*co*-PEG polymers were transformed into Mooney's representation that is classically used for rubbers.[40, 41, 48] Moreover, Mooney's representation from second tensile cycle will allow us to visualize hysteresis between loading and unloading cycle and help us to correlate with the cyclic compression data. As expected the peak Mooney's stress decreases with an increase in PEG concentration indicating the softening of the polymeric network. The Mooney's curve (Figure 6a) indicates that PGS and PGS-*co*-PEG polymers show limited hysteresis and all the samples return to their original shape after secession of tensile stress. The results also show that Mooney's stress for both PGS and PGS-*co*-PEG polymers reach a plateau phase within $1/\lambda_{\text{tens}} = 0.95$. This indicates that strain hardening of the polymer network occurs rapidly and the entire sample was under constant stress. This behavior highlights the elastomeric property of the copolymer network and highlights its usefulness in engineering scaffolds for a range of elastomeric tissues.

3.6 Cyclic Compressive Properties of PGS-*co*-PEG Polymers

The mechanical behavior polymeric network under unconfined cyclic compression can be used to evaluate the applicability of the copolymeric networks for soft tissue engineering. [46, 47] PGS and PGS-*co*-PEG polymers display elastomeric properties under compression, which is similar to our observations in tensile test (Figure 6b). The amount of energy absorbed by the PGS network was constant between first and fifth compressive cycles. Addition of 20 % of PEG significantly increases amount of energy absorbed. This might be due to deformation of swollen surfaces of the samples that does not return instantaneously to the original shape after cessation of compressive stress. Whereas, at higher PEG concentration (PGS-*co*-40PEG and PGS-*co*-60PEG), negligible hysteresis was observed and the network had high recoverability (>95%). This is mainly attributed to the formation of softer structures that are able to absorb energy during the loading cycle and release it almost completely during the unloading cycle.

In order to provide an easy comparison between uniaxial compression and uniaxial stretching we have used λ_{biax} as our deformation, since uniaxial compression is equivalent to biaxial stretching in terms of deformation.[42] The Mooney's representation, indicate that crosslinked network behave similarly in cyclic tensile and cyclic compression conditions. The rapid increase in Mooney's stress at smaller strain, indicate strain hardening of the polymeric network. The extent of strain hardening directly depends on the amount of PEG within the copolymer networks. Overall, PGS-*co*-PEG polymers exhibit unparalleled elastomeric properties that can be used to engineer a range of scaffolds for soft tissues that

are subjected to pulsating/cyclic mechanical forces such as blood vessels, cardiac, cartilage and muscle tissues.

3.7 Hydration Property of PGS-co-PEG Polymers

The hydration property of biomaterials is an important factor in determining their targeted applications for various biomedical and biological applications.[49-51] The addition of PEG within the hydrophobic backbone induces hydrophilic characteristic to the block copolymers.[39, 52] In the current approach, we expect that addition of PEG would facilitate uptake of water by the crosslinked network (Figure 7a). We first investigated surface characteristics of PGS and PGS-co-PEG polymers using optical tensiometry (goniometry) (Figure 7b). In this technique, a sessile water drop on the polymeric surface was observed and the contact angle was determined by measuring the angle between the polymer surface and a tangent to the water drop surface. Pure PGS shows a contact angle of $77.5 \pm 1.7^\circ$ with water. As expected, an increase in the PEG segment increases the hydrophilic nature. Addition of 60 % PEG to PGS reduces the contact angle to $66.2 \pm 0.1^\circ$.

The hydration properties of PGS and PGS-co-PEG polymers were further investigated by evaluating bulk hydration characteristic (Figure 7c). The crosslinked polymer samples were subjected to physiological conditions (37 °C and PBS) and uptake of water was monitored. The swelling study reveals the maximum water uptake within 48 hours for all PGS-co-PEG polymers, while PGS reaches the equilibrium water content (EWC) within 24 hours (Figure 7d). The EWC for PGS was 2.11 ± 0.88 whereas for PGS-co-60PEG was 32.98 ± 3.17 . Addition of 60 % PEG results in almost 15-fold increase in water uptake capacity. Moreover, as the PEG content in the block copolymer increases, the network becomes translucent in the swollen conditions, which is the characteristic of an amphiphilic copolymer network.

The hydration kinetics of PGS-co-PEG polymers was analyzed by fitting the initial hydration data ($W_t/W_{eq} < 0.6$) to Eq. (6). [51]

$$f = \frac{W_t}{W_{eq}} = K t^n \quad \text{Eq. (6)}$$

Where, 'K' is the characteristic swelling constant, 'n' is the hydration exponent that describes the mode of solvent transport, ' W_t ' is hydrated weight at time 't' and ' W_{eq} ' is saturated hydrated weight. For PGS, the characteristic swelling constant was not obtained due to a very low degree of swelling. While, the copolymer containing 20, 40 and 60 % PEG had characteristic swelling constants of 0.38, 0.41 and 0.5 respectively, indicating Fickian diffusion. Thus, the water transport through the polymeric network was diffusion limited and the relaxation of the copolymeric network had no significant interference with the solvent diffusion. This property is an asset for fabricating scaffolds with a controlled drug release properties.

3.8 In vitro Degradation of PGS-co-PEG Polymers

Chemical structures of polymeric materials play an important role in determining the degradation characteristic of the biomaterials.[13, 53] Moreover, the degradation rate and byproducts of degradation will determine the suitability of the polymeric materials for biomedical applications.[52, 54] PGS is a biodegradable polymer and is composed of glycerol and sebacic acid.[14] Glycerol is the basic building block of lipids and sebacic acid is a natural metabolic intermediate in ω -oxidation of various fatty acids.[21-23] Whereas, PEG is an inert and FDA-approved polymer that has been extensively used in designing various biomedical products and devices. Hence, it is expected that copolymer made from PEG and PGS can potentially be used for biological and biomedical applications.

In vitro degradation of PGS and PGS-co-PEG polymers was investigated under physiological conditions (PBS, 37 °C) for 21 days. All samples showed surface degradation characteristics (Figure 8a). All samples follow a linear mass loss and the rate of degradation increases with an increase in PEG concentration (Figure 8b). After 21 days, PGS showed 8.69±1.64 % mass loss, whereas PGS-co-20PEG, PGS-co-40PEG and PGS-co-60PEG indicate mass loss of 15.58±0.81 and 35.91±5.06 and 81.2±4.39 % respectively. The increase in degradation rate can be attributed to an increase in hydrophilicity of copolymer network with an increase in PEG concentration. The increase in hydrophilicity results in higher water uptake that accelerates the hydrolysis of PGS. This indicates that the slow degradation rate of PGS can be improved and tuned by incorporating PEG segments. The surface degradation characteristic combined with the diffusion controlled hydration kinetics of PGS-co-PEG polymers also suggests possible applications of PGS-co-PEG polymers elastomers for controlled drug release application.

3.9 Protein Adsorption and Cells-Matrix Interactions

The adsorption of protein on a biomaterial surface plays a significant role in controlling cell-matrix interactions.[33-35] The cell adhesion and spreading on a biomaterials surface is mediated by the presence of protein ad layer and the property of this ad layer is strongly influenced by the substrate chemistry and the composition of surrounding media. Under physiological conditions, the surrounding media contains a wide-range of proteins that are adsorbed on the biomaterial surface in competitive or sequential manner. Thus, it is important to investigate adsorption of protein on PGS-co-PEG surfaces. The effect of PEG concentration on protein adsorption was evaluated by immersion PGS and PGS-co-PEG in 10 % FBS at 37 °C for 24 hours. It is recognized that the protein adsorption is favored by a hydrophobic surfaces compared to a hydrophilic surfaces[55] and more than 60-70 % proteins in FBS are hydrophilic albumin.[56] The addition of PEG to PGS results in an increase in hydrophilicity of the polymeric network. The total amount of protein on PGS and PGS-co-PEG polymer surfaces was quantified and the results indicate that addition of PEG to PGS results in significant increase in amount of protein adsorption/absorption. This might be attributed to the absorption of proteins within the hydrated copolymer structure. These results support earlier finding that some of the hydrated and porous polymer structure facilitate protein absorption instead of protein adsorption.[56] To further investigate surface properties of the polymeric network, adsorption of cell adhesive proteins such as plasma fibronectin was determined. Plasma fibronectin is vital for initial cell attachment on the

biomaterials surface. The increase in PEG content within the copolymer network (PGS-*co*-20PEG, PGS-*co*-40PEG), reduces fibronectin adsorption compared to PGS (Figure 8c). In case of PGS-*co*-60PEG, an increase in fibronectin was observed. This was mainly attributed to high water uptake capacity of PGS-*co*-60PEG that results in fibronectin absorption.

To determine the feasibility of copolymer network for biomedical applications, preliminary study to evaluate cell-matrix interactions was performed. NIH/3T3 Fibroblasts were seeded on PGS and PGS-*co*-PEG polymer surfaces. Due to the autofluorescent of the PGS and PGS-*co*-PEG polymers, immunostaining images of the adhered cells were difficult to obtain. Therefore, we monitored the metabolic activity of adhered cells using Alamar Blue assay in low cell adhesion plates for 10 days (Figure 8d). Tissue culture polystyrene (TCPS) surface was used as a positive control. Compared to the positive control, the rate of proliferation of cells on PGS and PGS-*co*-PEG surfaces was almost half. However, no significant difference due to addition of PEG was observed on the copolymer network. The results suggest that PGS-*co*-PEG polymers support cell proliferation, rendering their use for various biomedical applications and regenerative medicine.

4. CONCLUSION

We successfully synthesized a range of PGS-*co*-PEG polymers by altering the molar ratios of glycerol to PEG. The incorporation of hydrophilic PEG chains results in increased water uptake of the copolymer network. The addition of PEG reduced the number of hydroxyl group within the copolymeric network and decreased crosslinking density after thermal curing process. PGS-*co*-PEG polymers show elastomeric properties and can be subjected to severe deformation such as bending and stretching without fracturing the structure. Under tension, PGS-*co*-PEG polymers displayed a unique stress-strain behavior that is typically observed in highly elastomeric soft tissues. The Young's modulus of PGS-*co*-PEG can be tuned from 13 kPa to 2.2 MPa by altering the amount of PEG within the network. Compared to PGS, more than six-fold increase in elongation was observed in PGS-*co*-60PEG. Similarly, under compression, addition of PEG results in soft and elastomeric network. Both surface and bulk characterization indicates that addition of PEG results in an increase in hydrophilicity of copolymeric network. The rate of degradation increases with an increase in PEG concentration, indicating that slow degradation rate of PGS can be improved. Moreover, PGS-*co*-60PEG support protein adsorption/absorption and cell proliferation, and thus can be used for a range of tissue engineering applications.

Acknowledgment

We would like to thank Dr. Shilpa Sant, and Hyeongho Shin for technical input and NMR experiment, respectively. AP would like to acknowledge postdoctoral fellowship (Fellowship No. PDF-388346-2010) awarded by Natural Science and Engineering Research Council, Canada. AKG would like to thank Prof. Robert Langer and MIT Portugal Program for financial support (MPP-09Call-Langer-47). GI would like to acknowledge Politecnico di Torino for financial support. HZ would like to acknowledge National Natural Science Fund for Distinguished Young Scholar (Grant No. 51025313). This research was funded by the US Army Engineer Research and Development Center, the Institute for Soldier Nanotechnology, the NIH (EB009196; DE019024; EB007249; HL099073; AR057837), and the National Science Foundation CAREER award (AK).

References

1. Langer R, Tirrell DA. Designing materials for biology and medicine. *Nature*. 2004; 428:487–492. [PubMed: 15057821]
2. Khademhosseini A, Vacanti JP, Langer R. Progress in tissue engineering. *Sci. Am.* 2009; 300:64–71. [PubMed: 19438051]
3. Slaughter BV, Khurshid SS, Fisher OZ, Khademhosseini A, Peppas NA. Hydrogels in regenerative medicine. *Adv. Mater.* 2009; 21:3307–3329. [PubMed: 20882499]
4. Fisher OZ, Khademhosseini A, Langer R, Peppas NA. Bioinspired materials for controlling stem cell fate. *Accounts Chem. Res.* 2010; 43:419–428.
5. Yoo J, Kuruvilla DJ, D'Mello SR, Salem AK, Bowden NB. New class of biodegradable polymers formed from reactions of an inorganic functional group. *Macromolecules.* 2012; 45:2292–2300. [PubMed: 22454554]
6. Athanasiou KA, Agrawal CM, Barber FA, Burkhart SS. Orthopaedic applications for PLA-PGA biodegradable polymers. *Arthroscopy.* 1998; 14:726–737. [PubMed: 9788368]
7. Patel A, Fine B, Sandig M, Mequanint K. Elastin biosynthesis: The missing link in tissue-engineered blood vessels. *Cardiovasc. Res.* 2006; 71:40–49. [PubMed: 16566911]
8. Jeong JH, Lim DW, Han DK, Park TG. Synthesis, characterization and protein adsorption behaviors of PLGA/PEG di-block co-polymer blend films. *Colloid Surface B.* 2000; 18:371–379.
9. Shi R, Chen D, Liu Q, Wu Y, Xu X, Zhang L, et al. Recent advances in synthetic bioelastomers. *Int. J. Mol. Sci.* 2009; 10:4223–4256. [PubMed: 20057942]
10. Liu X, Holzwarth JM, Ma PX. Functionalized synthetic biodegradable polymer scaffolds for tissue engineering. *Macromol. Biosci.* 2012; 12:911–919. [PubMed: 22396193]
11. Khan M, Ong ZY, Wiradharma N, Attia ABE, Yang Y-Y. Advanced materials for co-delivery of drugs and genes in cancer therapy. *Adv. Healthcare. Mater.* 2012; 1:373–392.
12. Li SM. Hydrolytic degradation characteristics of aliphatic polyesters derived from lactic and glycolic acids. *J. Biomed. Mater. Res.* 1999; 48:342–353. [PubMed: 10398040]
13. Nair LS, Laurencin CT. Biodegradable polymers as biomaterials. *Prog. Polym. Sci.* 2007; 32:762–798.
14. Wang Y, Kim YM, Langer R. *In vivo* degradation characteristics of poly(glycerol sebacate). *J. Biomed. Mater. Res. A.* 2003; 66A:192–197. [PubMed: 12833446]
15. Rai R, Tallawi M, Grigore A, Boccaccini AR. Synthesis, properties and biomedical applications of poly(glycerol sebacate) (PGS): A review. *Prog. Polym. Sci.* 2012; 37:1051–1078.
16. Wang YD, Ameer GA, Sheppard BJ, Langer R. A tough biodegradable elastomer. *Nat. Biotechnol.* 2002; 20:602–606. [PubMed: 12042865]
17. Chen QZ, Bismarck A, Hansen U, Junaid S, Tran MQ, Harding SE, et al. Characterisation of a soft elastomer poly(glycerol sebacate) designed to match the mechanical properties of myocardial tissue. *Biomaterials.* 2008; 29:47–57. [PubMed: 17915309]
18. Jaafar IH, Ammar MM, Jedlicka SS, Pearson RA, Coulter JP. Spectroscopic evaluation, thermal, and thermomechanical characterization of poly(glycerol-sebacate) with variations in curing temperatures and durations. *J. Mater. Sci.* 2010; 45:2525–2529.
19. Sun ZJ, Sun CW, Sun B, Lu XL, Dong DL. The polycondensing temperature rather than time determines the degradation and drug release of poly(glycerol-sebacate) doped with 5-fluorouracil. *J. Biomat. Sci-Polym. E.* 2012; 23:833–841.
20. Sun ZJ, Chen C, Sun MZ, Ai CH, Lu XL, Zheng YF, et al. The application of poly (glycerol-sebacate) as biodegradable drug carrier. *Biomaterials.* 2009; 30:5209–5214. [PubMed: 19560817]
21. Liu GY, Hinch B, Beavis AD. Mechanisms for the transport of alpha,omega-dicarboxylates through the mitochondrial inner membrane. *J. Biol. Chem.* 1996; 271:25338–25344. [PubMed: 8810298]
22. Grego AV, Mingrone G. Dicarboxylic acid, an alternate fuel substrate in parenteral nutrition -an update. *Clin. Nutr.* 1995; 14:143–148. [PubMed: 16843924]

23. Mortensen PB, Gregersen N. The biological origin of ketotic dicarboxylic aciduria-*in vivo* and *in vitro* investigations of the omega-oxidation of C6-C16-monocarboxylic acid in unstarved, starved and diabetic rats. *Biochim. Biophys. Acta.* 1981; 666:394–404. [PubMed: 6798996]
24. Chen QZ, Bismarck A, Hansen U, Junaid S, Tran MQ, Harding SE, et al. Characterisation of a soft elastomer poly (glycerol sebacate) designed to match the mechanical properties of myocardial tissue. *Biomaterials.* 2008; 29:47–57. [PubMed: 17915309]
25. Motlagh D, Yang J, Lui KY, Webb AR, Ameer GA. Hemocompatibility evaluation of poly (glycerol-sebacate) *in vitro* for vascular tissue engineering. *Biomaterials.* 2006; 27:4315–4324. [PubMed: 16675010]
26. Kempainen JM, Hollister SJ. Tailoring the mechanical properties of 3D-designed poly (glycerol sebacate) scaffolds for cartilage applications. *J. Biomed. Mater. Res. A.* 2010; 94:9–18. [PubMed: 20091702]
27. Sundback CA, Shyu JY, Wang Y, Faquin WC, Langer RS, Vacanti JP, et al. Biocompatibility analysis of poly (glycerol sebacate) as a nerve guide material. *Biomaterials.* 2005; 26:5454–5464. [PubMed: 15860202]
28. Pritchard CD, Arnér KM, Langer RS, Ghosh FK. Retinal transplantation using surface modified poly (glycerol-co-sebacic acid) membranes. *Biomaterials.* 2010; 31:7978–7984. [PubMed: 20656341]
29. Sant S, Iyer D, Gaharwar AK, Patel A, Khademhosseini A. Effect of biodegradation and de novo matrix synthesis on the mechanical properties of VIC-seeded PGS-PCL scaffolds. *Acta. Biomater.* 2013 DOI: 10.1016/j.actbio.2012.11.014.
30. Sant S, Hwang CM, Lee S-H, Khademhosseini A. Hybrid PGS–PCL microfibrinous scaffolds with improved mechanical and biological properties. *J. Tissue. Eng. Regen. M.* 2011; 5:283–291. [PubMed: 20669260]
31. Sun ZJ, Wu L, Huang W, Zhang XL, Lu XL, Zheng YF, et al. The influence of lactic on the properties of Poly (glycerol-sebacate-lactic acid). *Mat. Sci. Eng. C-Biomim.* 2009; 29:178–182.
32. Chu CC. The *in vitro* degradation of poly(glycolic acid) sutures -effect of pH. *J. Biomed. Mater. Res.* 1981; 15:795–804. [PubMed: 6273445]
33. Huebsch N, Mooney DJ. Inspiration and application in the evolution of biomaterials. *Nature.* 2009; 462:426–432. [PubMed: 19940912]
34. Place ES, Evans ND, Stevens MM. Complexity in biomaterials for tissue engineering. *Nat. Mater.* 2009; 8:457–470. [PubMed: 19458646]
35. Drury JL, Mooney DJ. Hydrogels for tissue engineering: scaffold design variables and applications. *Biomaterials.* 2003; 24:4337–4351. [PubMed: 12922147]
36. Mihaila SM, Gaharwar AK, Reis RL, Marques AP, Gomes ME, Khademhosseini A. Photocrosslinkable kappa-carrageenan hydrogels for tissue engineering applications. *Adv. Healthcare Mater.* DOI:10.1002/adhm.201200317.
37. Liu Q-Y, Wu S-Z, Tan T-W, Weng J-Y, Zhang L-Q, Liu L, et al. Preparation and properties of a novel biodegradable polyester elastomer with functional groups. *J. Biomat. Sci-Polym. E.* 2009; 20:1567–1578.
38. Penco M, Marcioni S, Ferruti P, Dantone S, Deghenghi R. Degradation behaviour of block copolymers containing poly(lactic-glycolic acid) and poly(ethylene glycol) segments. *Biomaterials.* 1996; 17:1583–1590. [PubMed: 8842362]
39. Martina M, Hutmacher DW. Biodegradable polymers applied in tissue engineering research: a review. *POLYM INT.* 2007; 56:145–157.
40. Flory, PJ. Principles of polymer chemistry. Cornell University Press; Ithaca, NY: 1953.
41. Akagi Y, Katashima T, Katsumoto Y, Fujii K, Matsunaga T, Chung U-i, et al. Examination of the theories of rubber elasticity using an ideal polymer network. *Macromolecules.* 2011; 44:5817–5821.
42. Webber RE, Creton C. Large strain hysteresis and mullins effect of tough double-network hydrogels. *Macromolecules.* 2007; 40:2919–2927.
43. Nakano K, Sugawara M, Ishihara K, Kanazawa S, Corin WJ, Denslow S, et al. Myocardial stiffness derived from end-systolic wall stress and logarithm of reciprocal of wall thickness.

- Contractility index independent of ventricular size. *Circulation*. 1990; 82:1352–1361. [PubMed: 2401069]
44. Chen Q-Z, Harding SE, Ali NN, Lyon AR, Boccaccini AR. Biomaterials in cardiac tissue engineering: Ten years of research survey. *Mat. Sci. Eng. R*. 2008; 59:1–37.
 45. Athanasiou KA, Agarwal A, Dzida FJ. Comparative study of the intrinsic mechanical properties of the human acetabular and femoral head cartilage. *J. Orthop. Res.* 1994; 12:340–349. [PubMed: 8207587]
 46. Gaharwar AK, Dammu SA, Canter JM, Wu C-J, Schmidt G. Highly extensible, tough, and elastomeric nanocomposite hydrogels from poly(ethylene glycol) and hydroxyapatite nanoparticles. *Biomacromolecules*. 2011; 12:1641–1650. [PubMed: 21413708]
 47. Gaharwar AK, Rivera CP, Wu C-J, Schmidt G. Transparent, elastomeric and tough hydrogels from poly(ethylene glycol) and silicate nanoparticles. *Acta. Biomater.* 2011; 7:4139–4148. [PubMed: 21839864]
 48. Katti DS, Lakshmi S, Langer R, Laurencin CT. Toxicity, biodegradation and elimination of polyanhydrides. *Adv. Drug. Deliver. Rev.* 2002; 54:933–961.
 49. Chen S, Li L, Zhao C, Zheng J. Surface hydration: Principles and applications toward low-fouling/nonfouling biomaterials. *Polymer*. 2010; 51:5283–5293.
 50. Gaharwar AK, Kishore V, Rivera C, Bullock W, Wu C-J, Akkus O, et al. Physically crosslinked nanocomposites from silicate-crosslinked PEO: Mechanical properties and osteogenic differentiation of human mesenchymal stem cells. *Macromol. Biosci.* 2012; 12:779–793. [PubMed: 22517665]
 51. Gaharwar AK, Schexnailder PJ, Kline BP, Schmidt G. Assessment of using laponite® cross-linked poly(ethylene oxide) for controlled cell adhesion and mineralization. *Acta Biomater.* 2011; 7:568–577. [PubMed: 20854941]
 52. Mohanty AK, Misra M, Hinrichsen G. Biofibres, biodegradable polymers and biocomposites: An overview. *Macromol. Mater. Eng.* 2000; 276-277:1–24.
 53. Göpferich A. Mechanisms of polymer degradation and erosion. *Biomaterials*. 1996; 17:103–114. [PubMed: 8624387]
 54. Taylor MS, Daniels AU, Andriano KP, Heller J. 6 Bioabsorbable polymers - *in vitro* acute toxicity of accumulated degradation products. *J. Appl. Biomater.* 1994; 5:151–157. [PubMed: 10147175]
 55. Mequanint K, Patel A, Bezuidenhout D. Synthesis, swelling behavior, and biocompatibility of novel physically cross-linked polyurethane-block-poly(glycerol methacrylate) hydrogels. *Biomacromolecules*. 2006; 7:883–891. [PubMed: 16529427]
 56. Patel A, Mequanint K. Synthesis and characterization of polyurethane-block-poly(2-hydroxyethyl methacrylate) hydrogels and their surface modification to promote cell affinity. *J. Bioact. Compat. Pol.* 2011; 26:114–129.

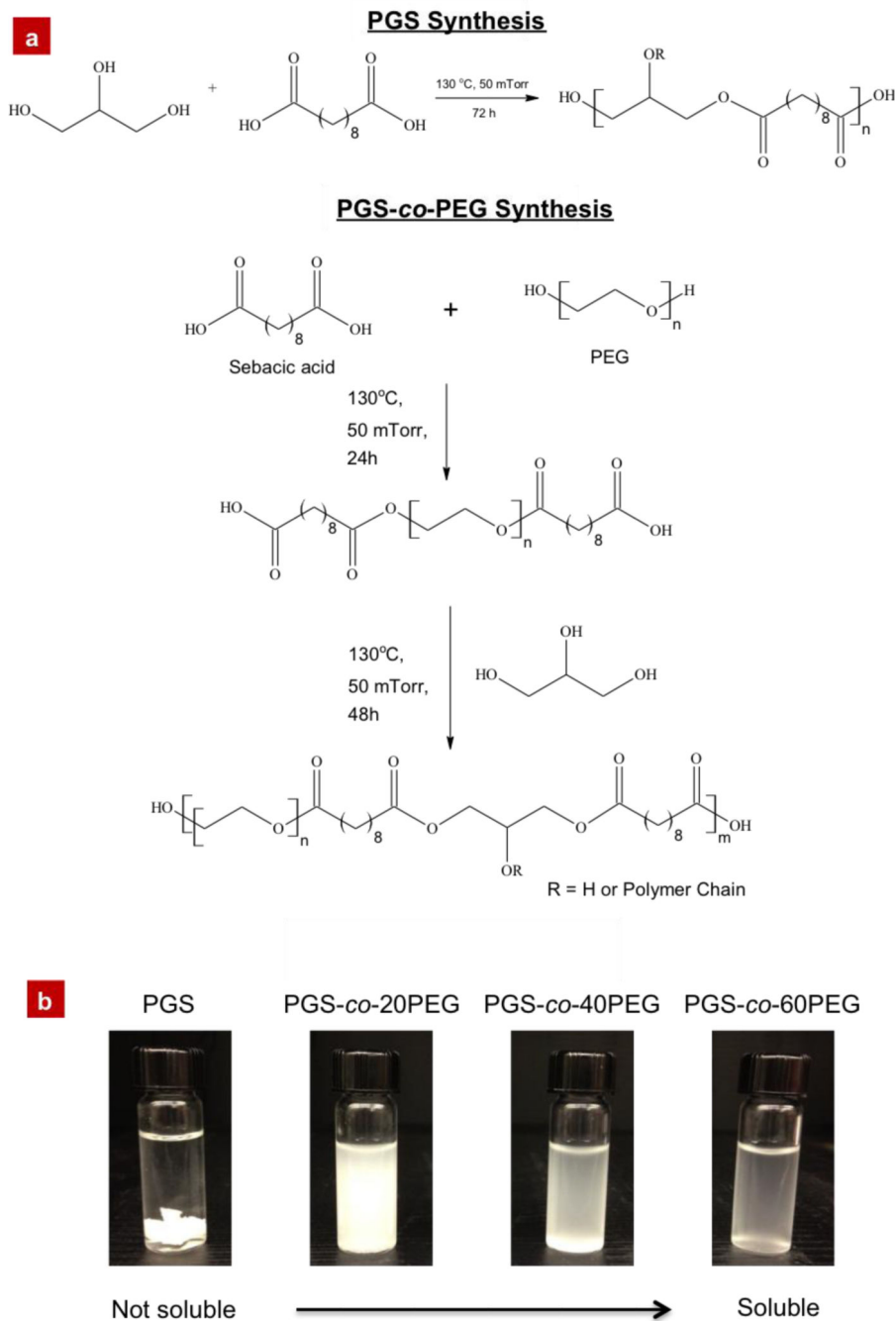


Figure 1. Synthesis of PGS and PGS-co-PEG polymers

(a) PGS was synthesized by polycondensation of equimolar glycerol and sebacic acid. The synthesis of PGS-co-PEG polymers involves polycondensation of PEG and sebacic acid to obtain a linear polymer chain, followed by addition of glycerol to obtain a block copolymer of PGS-co-PEG. The ratio of glycerol to PEG was altered to obtain copolymer with different degree of amphiphilicity. (b) The addition of PEG reduces available hydroxyl group on copolymer network and increases hydrophilicity of PGS-co-PEG copolymers. The increase in PEG concentration renders dissolution of copolymer in water.

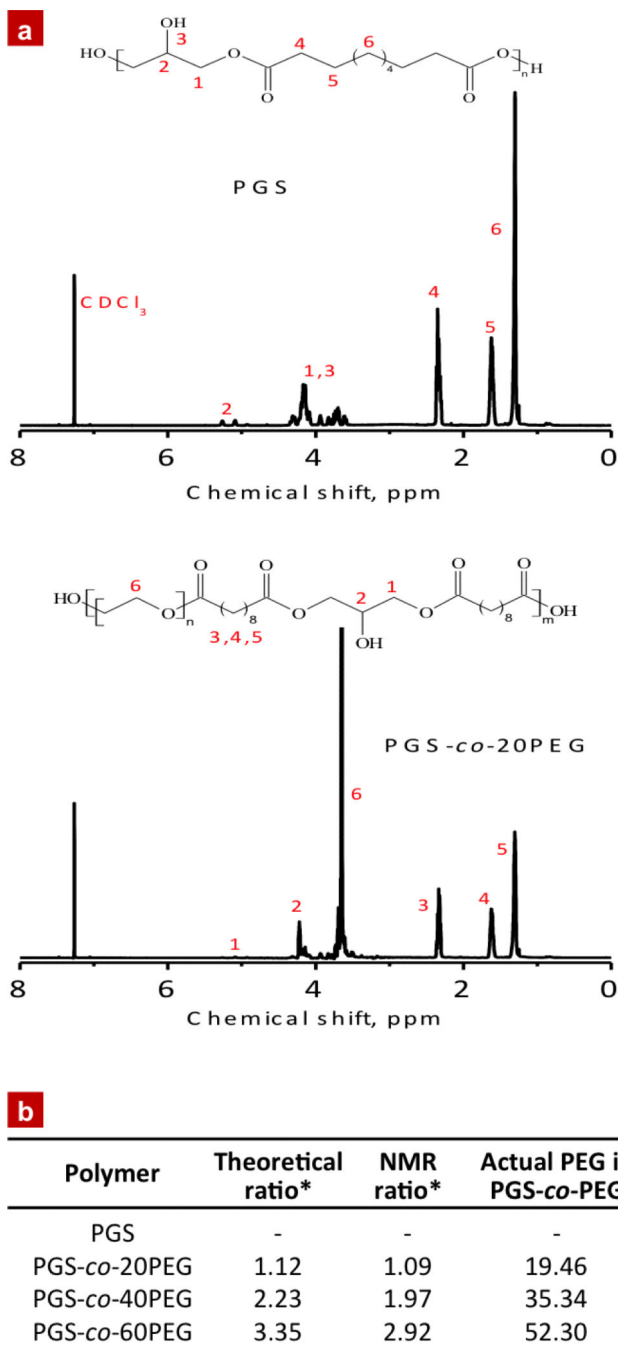


Figure 2. $^1\text{H-NMR}$ spectra of PGS and PGS-co-20PEG polymers

The methylene peaks related to sebacic acid were recognized at 1.30, 1.62 and 2.35 ppm, whereas peaks between 4.05-4.35 ppm and 5.05-5.30 ppm were detected for glycerol. The presence of an additional methylene peak from PEG segment was observed in the ^1H NMR spectra of PGS-co-PEG polymers, indicating the presence of PEG segment within prepolymer solution. (b) NMR ratio between PGS and PEG was calculated by determining ratio between methylene hydrogen within PEG and sebacic acid that correlates well with the theoretical estimation indicating close control over the polymer synthesis process.

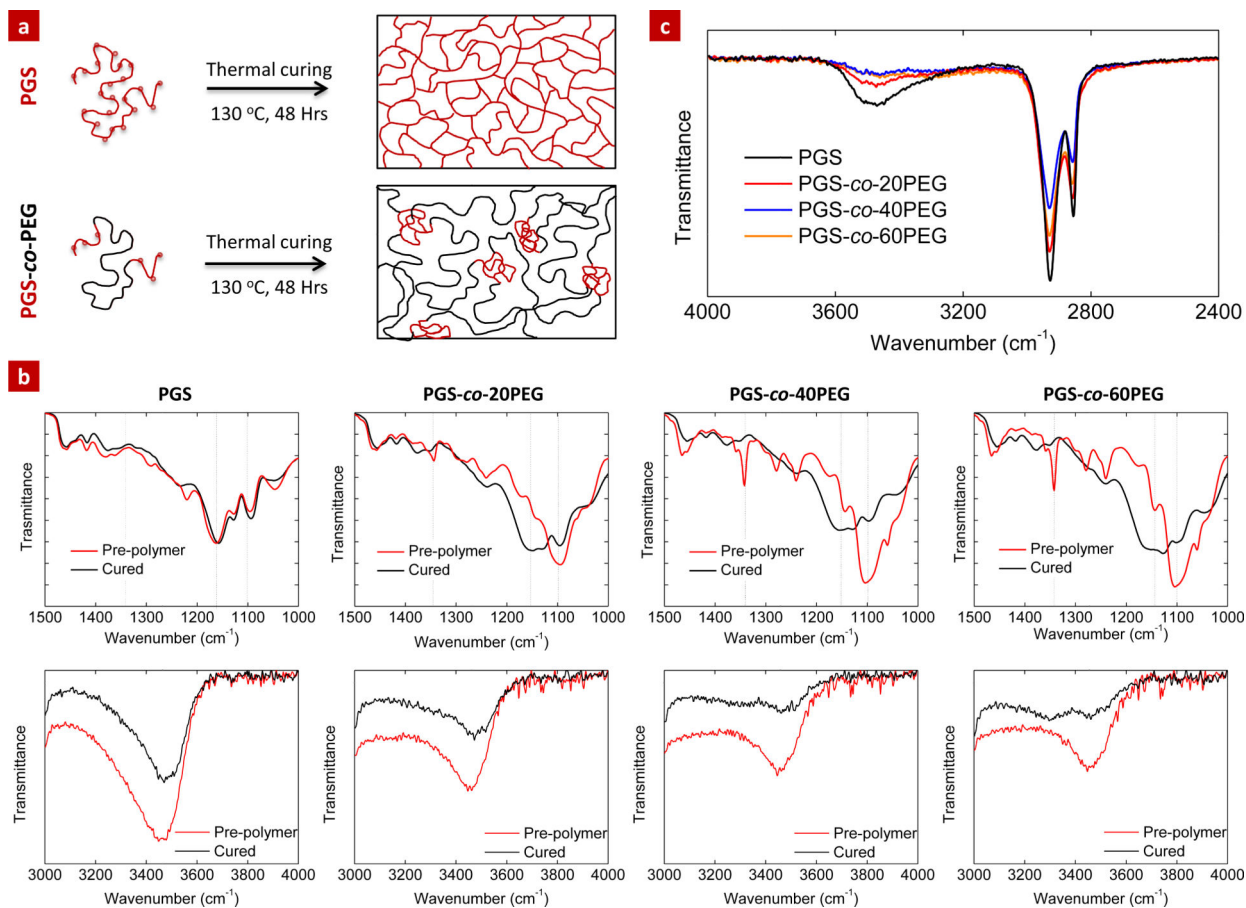


Figure 3. Thermal crosslinking of PGS-co-PEG polymer network

(a) Schematic showing crosslinking of pure PGS results in formation of highly crosslinked network due to presence of hydroxyl group on PGS backbone. The addition of PEG to PGS significantly reduces the crosslinking density due to decrease in number of hydroxyl group. (b) The FTIR spectra of PGS and PGS-co-PEG polymers (20, 40 and 60% PEG) were obtained before and after the thermal crosslinking process. The decrease in carboxyl (COOH), and hydroxyl (OH) group at 1350 and 1100 (and at 3400) cm⁻¹ respectively and increase in ester (COO) at 1150 cm⁻¹ indicates thermal crosslinking of PGS. (c) FTIR spectra of PGS and PGS-co-PEG polymers (20%, 40% and 60% PEG) after curing indicate that the CH₂/OH peak ratio increases.

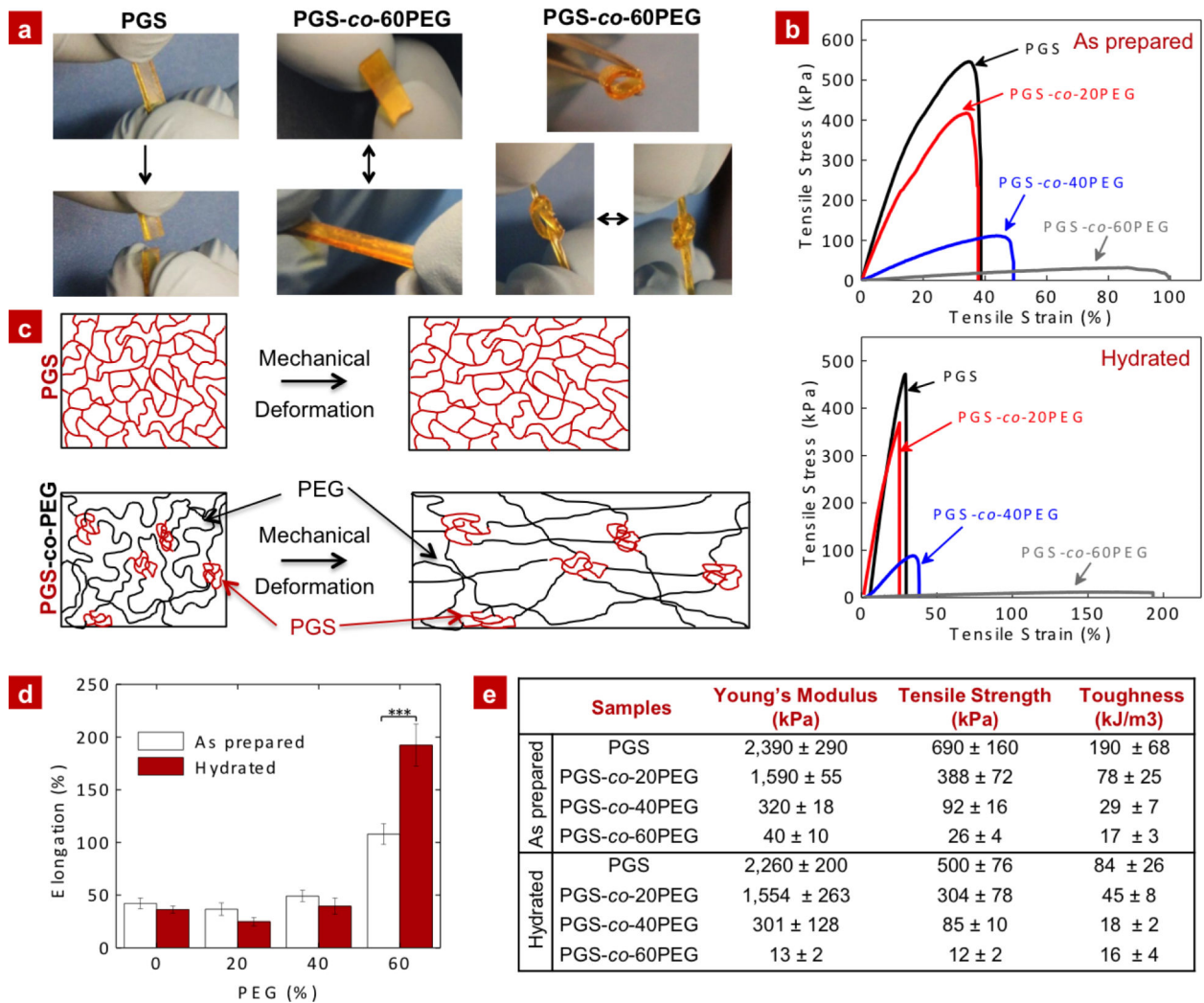


Figure 4. Tensile properties of PGS-co-PEG polymers

(a) PGS-co-PEG polymer can be subjected to serve deformation such as bending, knotting, and stretching without fracturing the structure. (b) The stress-strain curves for as prepared and hydrated PGS and PGS-co-PEG polymers were represented. (c) Thermal curing results in densely crosslinked network, whereas addition of PEG results in lower crosslinked network that results in elongation and deformation of polymeric network. (d) No significant difference in elongation was detected in as prepared and hydrated samples of PGS, PGS-co-20PEG and PGS-co-40PEG polymers. The addition of 60% PEG results in more than six-fold increase in elongation compared to pure PGS. In hydrated conditions, PGS-co-60PEG polymer results in significant increase elongation due to higher chain flexibility during mechanical deformation. (e) The table summarizing Young's modulus, tensile strength and toughness of PGS and PGS-co-PEG polymers from the stress-strain curve. The bars represent mean \pm standard deviation ($n=5$), (***) $p < 0.001$, ANOVA with Tukey's multiple comparison test).

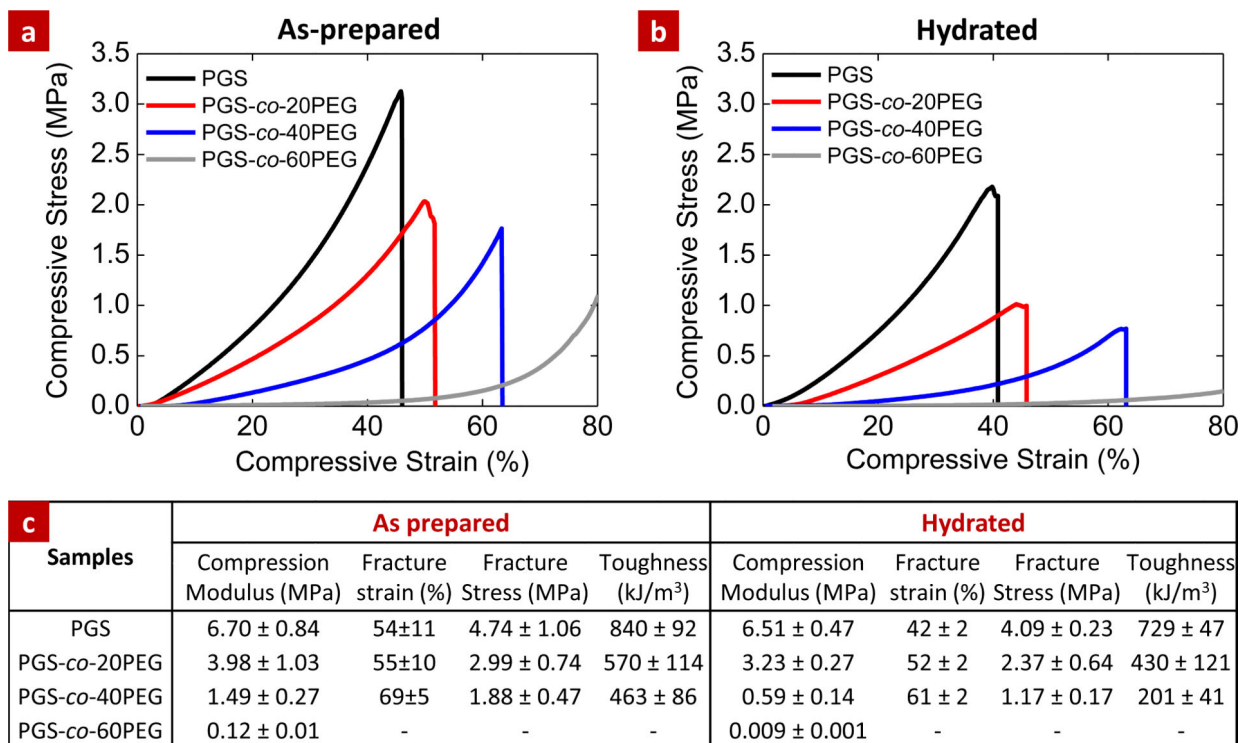


Figure 5. Compressive properties of PGS-co-PEG polymers

An unconfined compression test was used to determine the compressive properties of PGS and PGS-co-PEG polymers in (a) as prepared and (b) hydrated conditions. The compressive properties such as modulus, fracture strain, fracture stress and toughness were calculated from the stress-strain curves (c). Addition of PEG results in decrease in the compressive modulus of PGS-co-PEG polymers compared to PGS. In hydrated conditions, a significant decrease in mechanical properties was observed in PGS-co-PEG polymers. This can be mainly attributed to an increase in the water uptake ability of the copolymer at higher PEG content. The data represented as mean ± standard deviation (n=5).

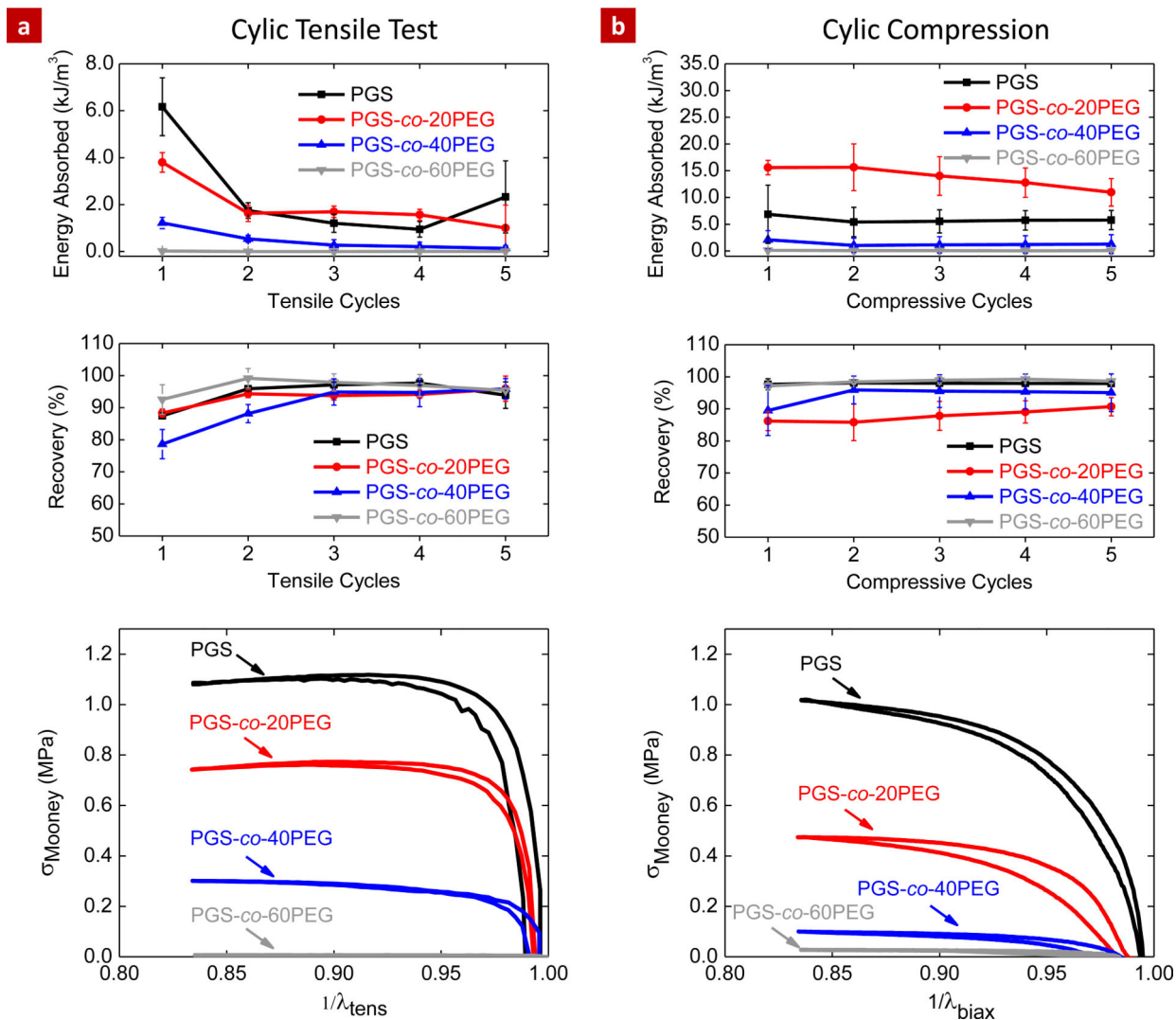


Figure 6. Cyclic tensile and compressive properties of PGS-co-PEG polymers

The elastomeric properties of the copolymeric network were investigated under (a) cyclic tensile and (b) cyclic compression conditions. The fully hydrated samples were subjected to cyclic strain and the loading and unloading curves were monitored for five consecutive cycles. Both, PGS and PGS-co-PEG polymers showed highly elastomeric characteristic in tensile and compression. All the copolymeric network display a plateau in energy absorbed and recovery of the network after the first cycle indicating elastomeric properties. Mooney's representation from second cycle was used to visualize hysteresis between loading and unloading cycle. The Mooney's stress decreases with an increase in PEG concentration indicating the softening of the polymeric network. The Mooney's curve indicates that PGS and PGS-co-PEG polymers show very limited hysteresis and all the samples return to their original shape after secession of tensile stress. The data represented as mean \pm standard deviation (n=5).

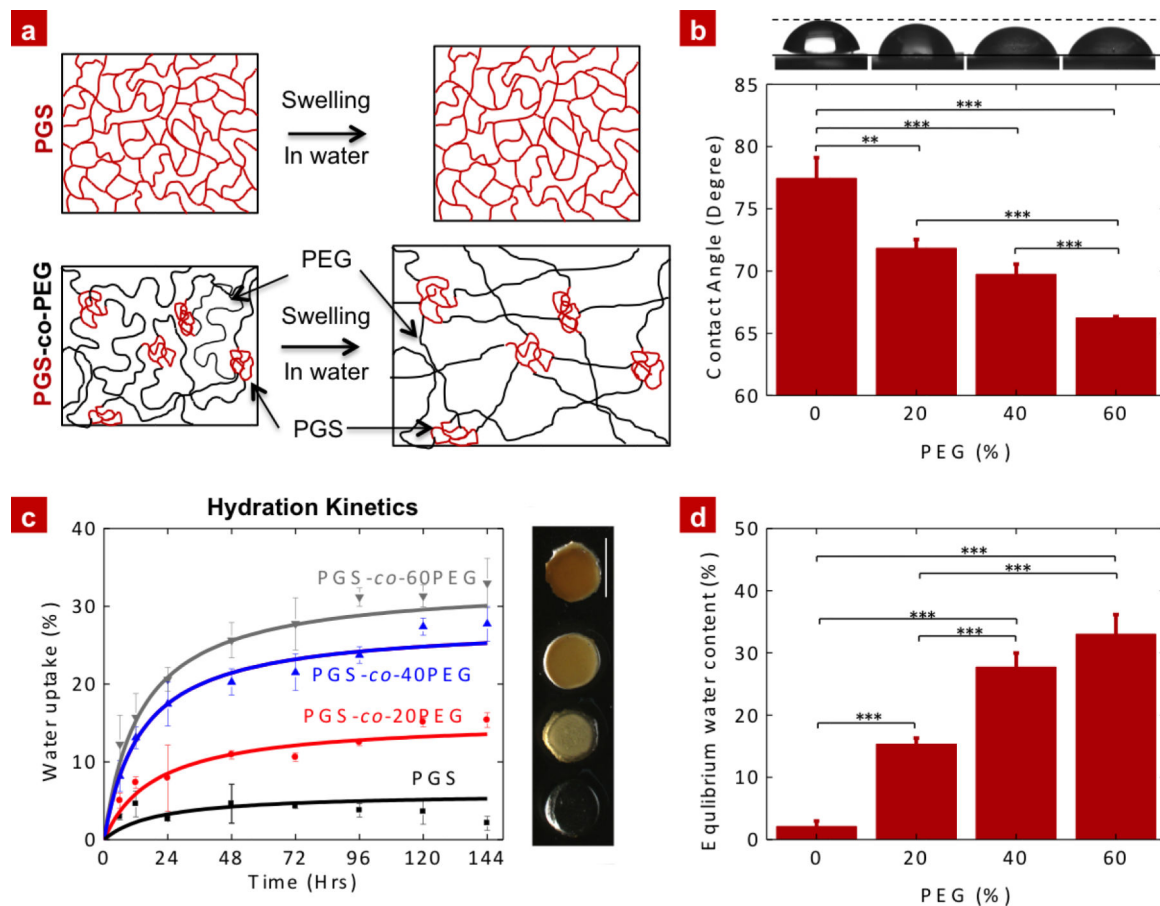


Figure 7. Effect of PEG on hydrophilicity of PGS-co-PEG polymers

(a) Schematic showing addition of PEG to PGS results in a decrease in crosslinking density and water readily adsorbed by PEG present in PGS-co-PEG polymers. (b) The contact angle measurements indicate an increase in surface hydrophilicity due to addition of PEG as determined by the decrease in contact angle of water on PGS-co-PEG polymers. (c) The hydration kinetic of PGS-co-PEG copolymers strongly depends on the amount of PEG within the network. All the copolymer reaches saturated hydration degree within 72 hours. (d) The equilibrium water content significantly increases with an increase in PEG concentration. The data represented as mean \pm standard deviation ($n=5$) (** $p<0.01$, *** $p<0.001$, ANOVA with Tukey's multiple comparison test).

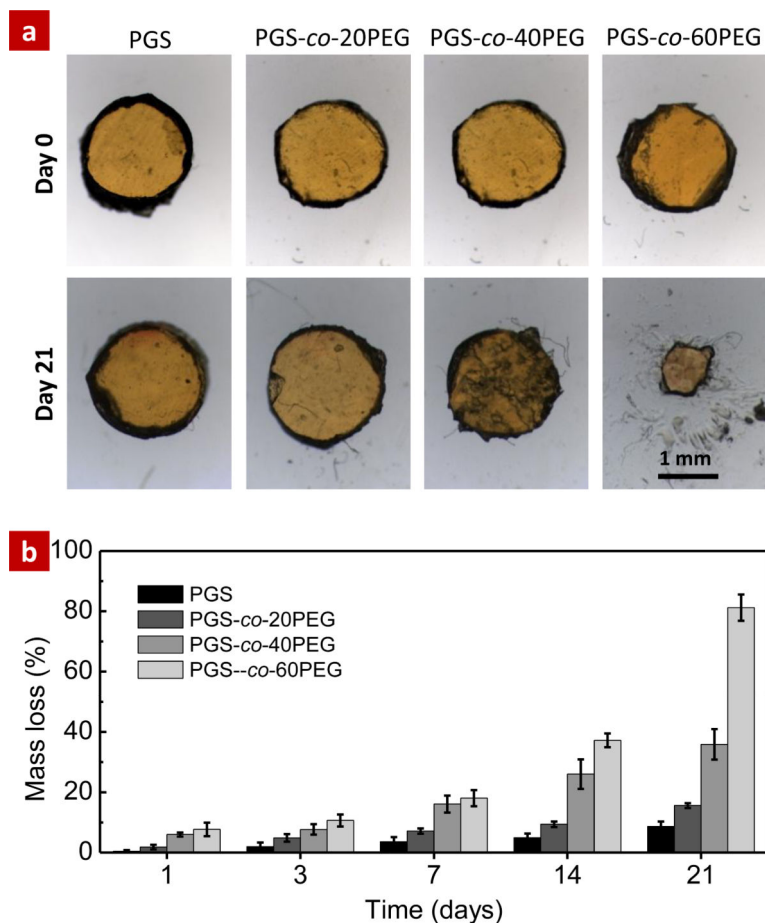


Figure 8. The physiological stability of copolymeric network determined by *in vitro* degradation of PGS-co-PEG polymers under physiological conditions (PBS, 37 °C)

(a) The optical images of copolymer network at day 0 and day 21 demonstrate that PGS and PGS-co-PEG polymer degrades via surface erosion mechanism. (b) The weight loss of polymeric network was monitored over the period of 21 days. The increase in hydrophilicity due to addition of PGS results in higher water uptake that accelerates the hydrolysis of PGS. The degradation rate directly depends on the amount of PEG within the PGS-co-PEG polymers network. The data represented as mean \pm standard deviation (n=5). Two-way ANOVA indicates significant ($p < 0.0001$) effect of composition and time on the mass loss of polymeric network.

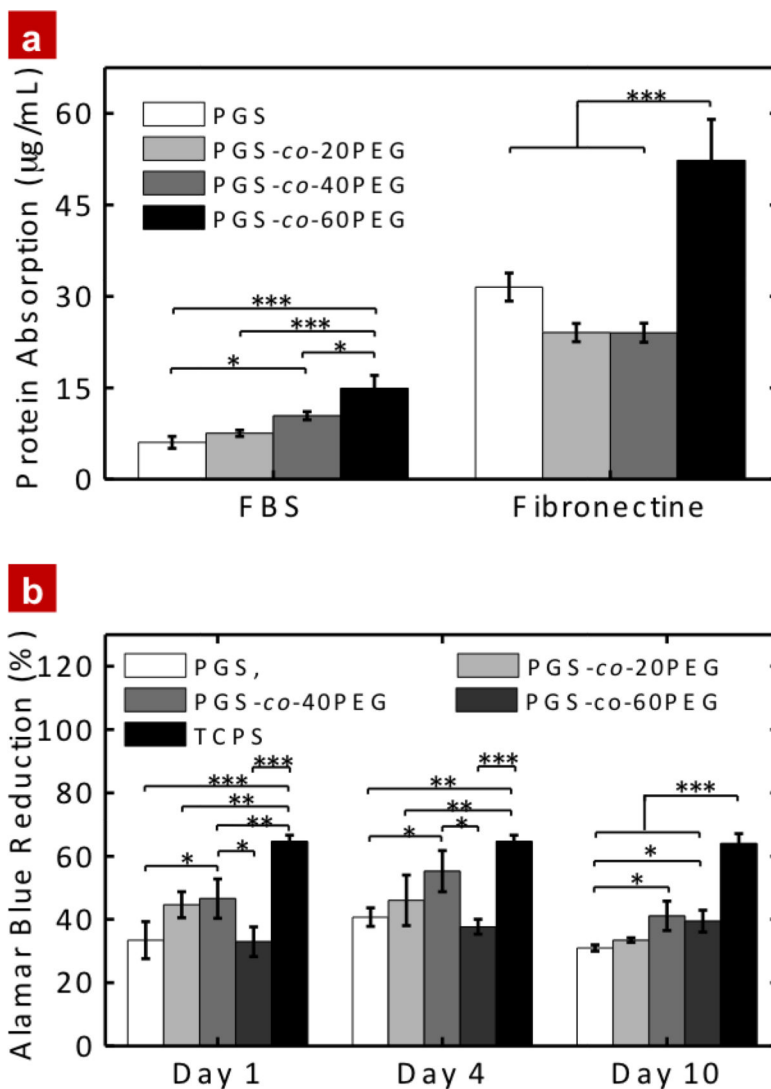


Figure 9. Protein adsorption and *in vitro* cell proliferation on PGS and PGS-co-PEG polymers (a) The protein adsorption/absorption on polymeric surface was determined using fetal bovine serum (FBS) and fibronectin. The addition of PEG to PGS, significantly increase adsorption/absorption of protein due to hydration of copolymer structure. (d) Proliferation of NIH 3T3 cells on PGS and PGS-co-PEG polymers was evaluated using Alamar Blue assay. Tissue culture polystyrene (TCPS) surface was used as a positive control. Both PGS and PGS-co-PEG polymers support cell proliferation. The data represented as mean \pm standard deviation (n=3) (**p<0.01, ***p<0.001, ANOVA with Tukey's multiple comparison test).